

Supporting Information

2D/1D PbI₂/Sb₂S₃ van der Waals Heterojunction for Highly Sensitive and Broadband Photodetectors

Shili Fu ^{1,†}, Xiaohui Liu ^{1,†}, Jiaxiu Man ¹, Quanhong Ou ¹, Xiaolu Zheng ¹, Zhiyong Liu ^{1,2}, Ting Zhu ^{1,2,*}, Hong-En Wang ^{1,2,*}

¹ College of Physics and Electronic Information, Yunnan Normal University, 650500 Kunming, Yunnan, China. E-mail: hongen.wang@ynnu.edu.cn; zhut0002@ynnu.edu.cn

² Yunnan Key Laboratory of Optoelectronic Information Technology, Key Laboratory of Advanced Technique & Preparation for Renewable Energy Materials, Ministry of Education, Yunnan Normal University, 650500 Kunming, Yunnan, China. E-mail: hongen.wang@outlook.com

[†] Shili Fu and Xiaohui Liu contributed equally to this work.

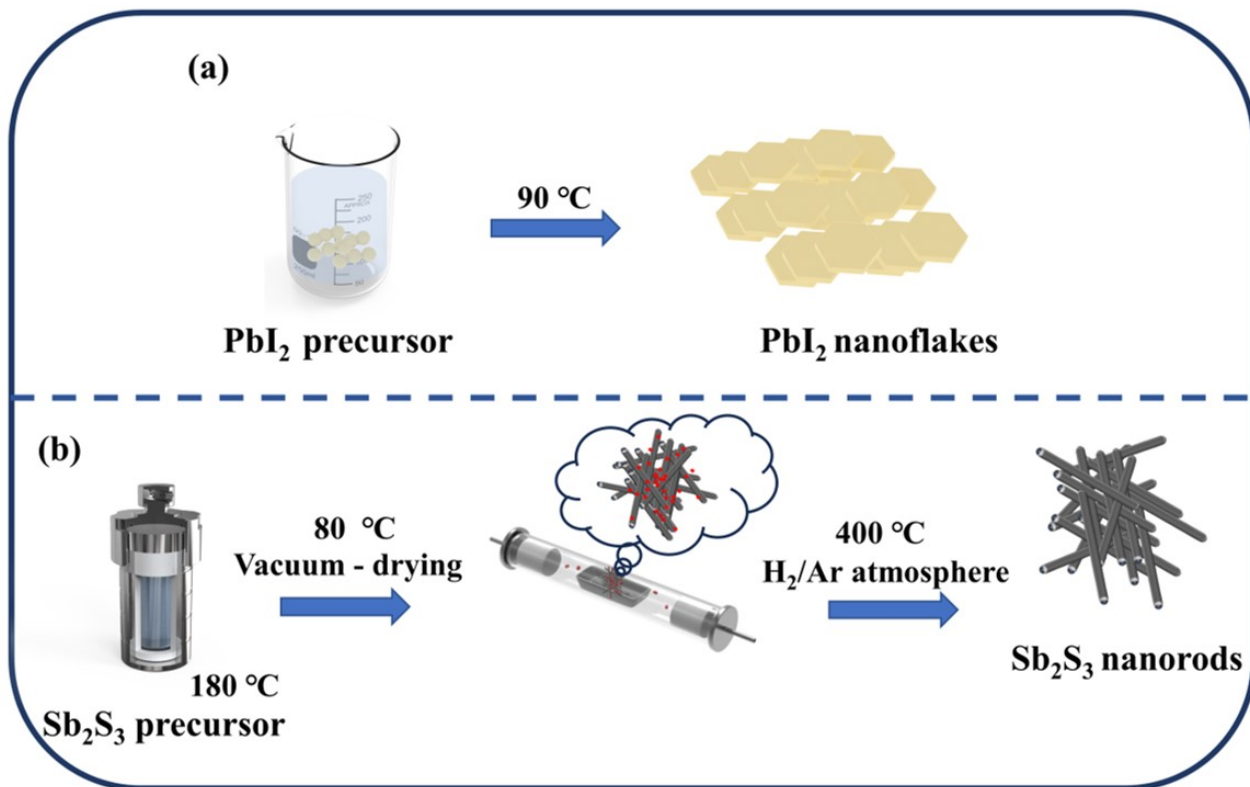


Figure S1. Schematic synthesis routes of (a) PbI_2 nanosheets and (b) Sb_2S_3 microrods, respectively.

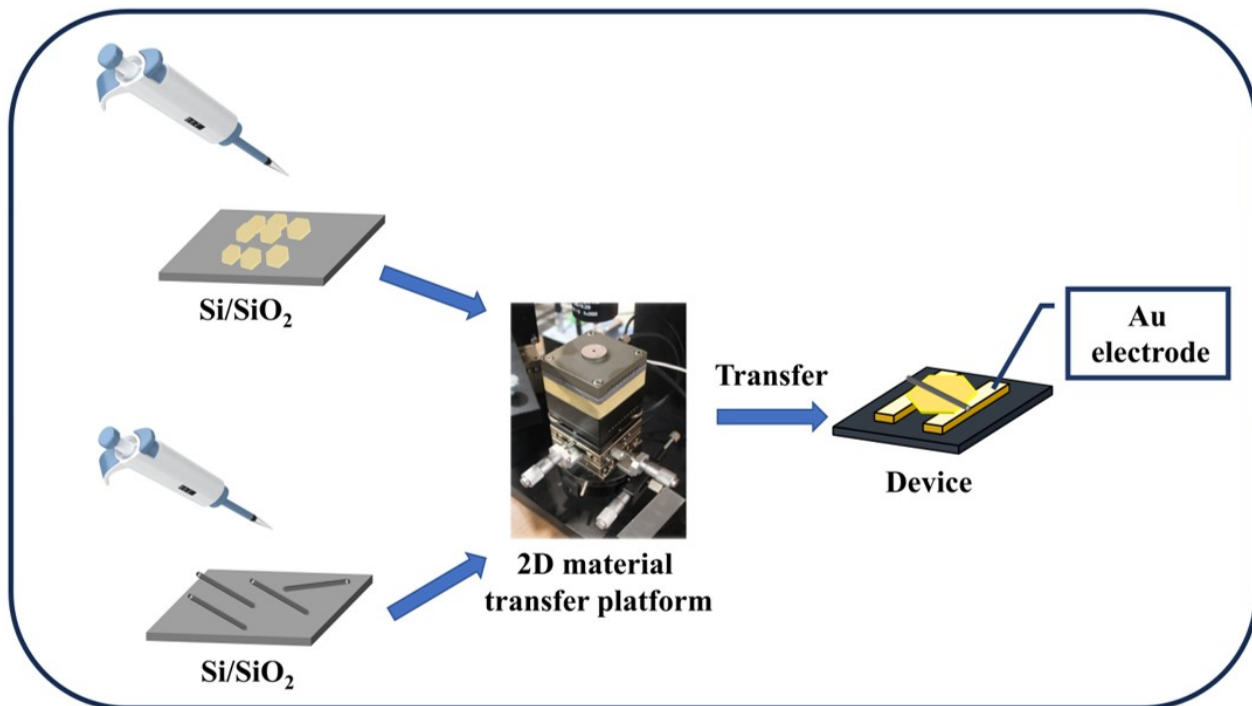


Figure S2. Schematic fabrication procedure of the 2D/1D PbI₂/Sb₂S₃ heterojunction device.

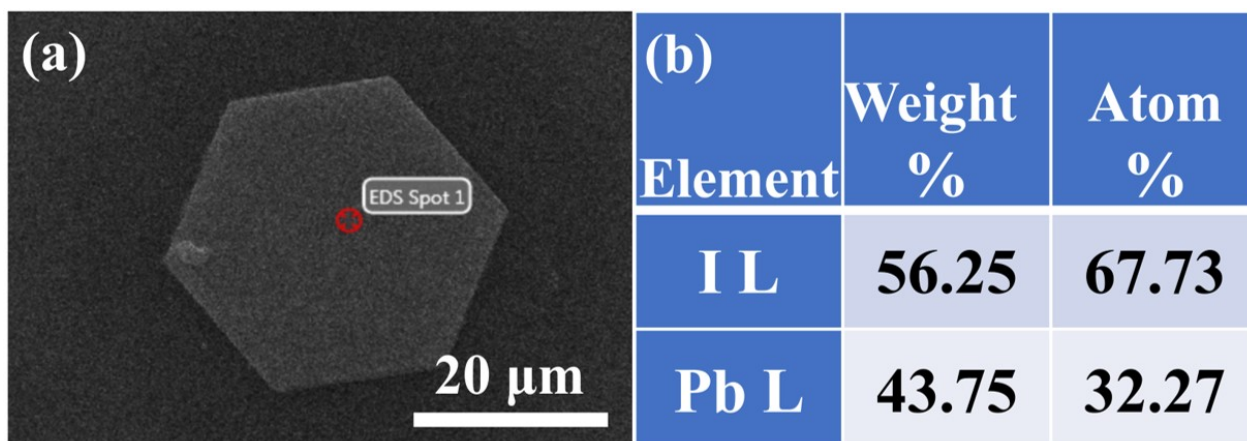
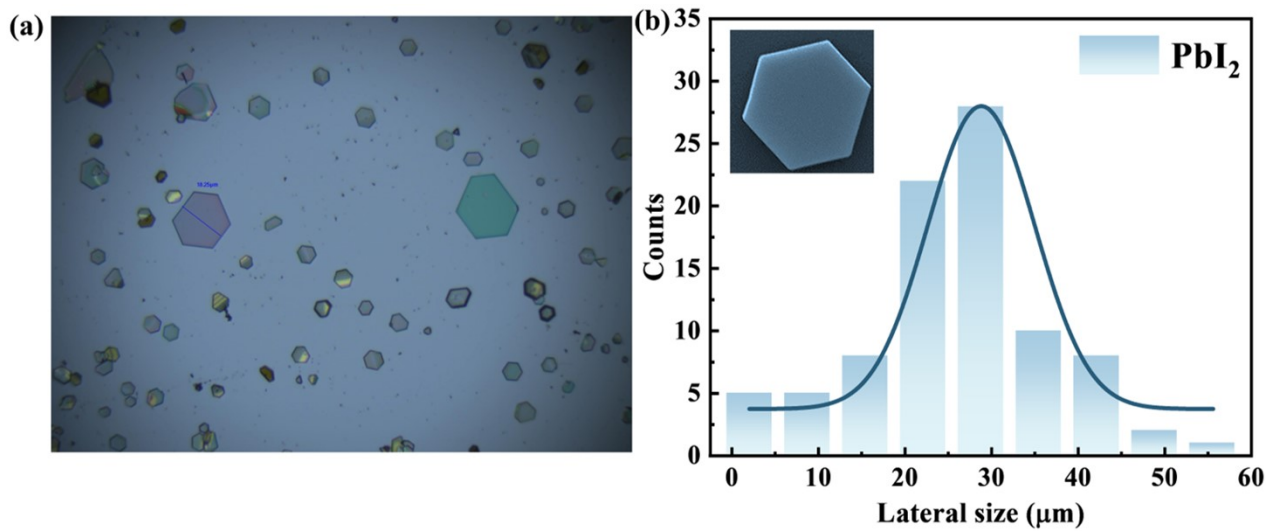


Figure S3. SEM image of a PbI₂ nanosheet (a) and corresponding EDX analysis result of I and Pb elements (b) from a spot selected from the near center region (red circle), showing the atomic ratio of Pb : I is near to 1 : 2.



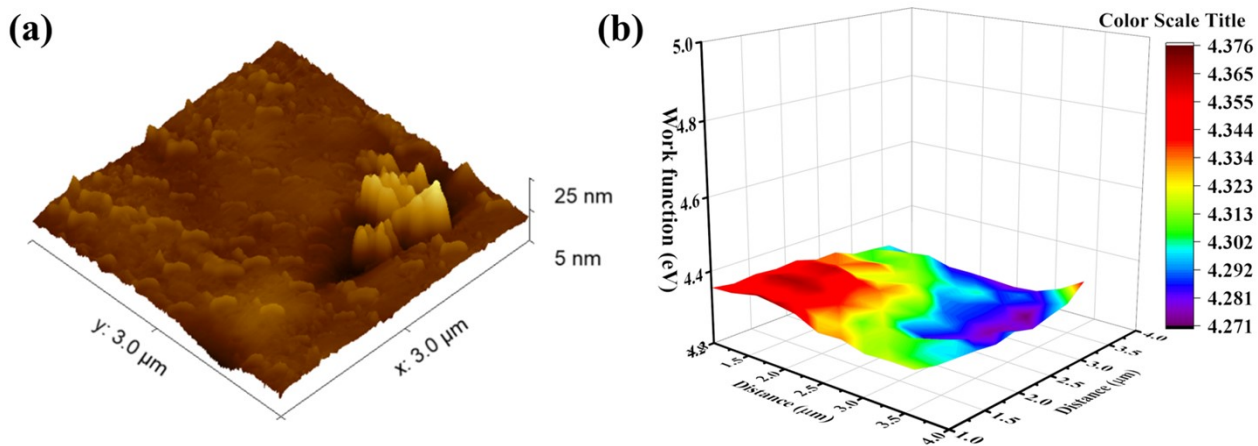


Figure S5. (a) AFM and (b) KPFM images of a selected rectangular area with a size of $3 \times 3 \mu\text{m}^2$ from a PbI_2 nanosheet, validating its relatively uniform surface and surface work function distribution.

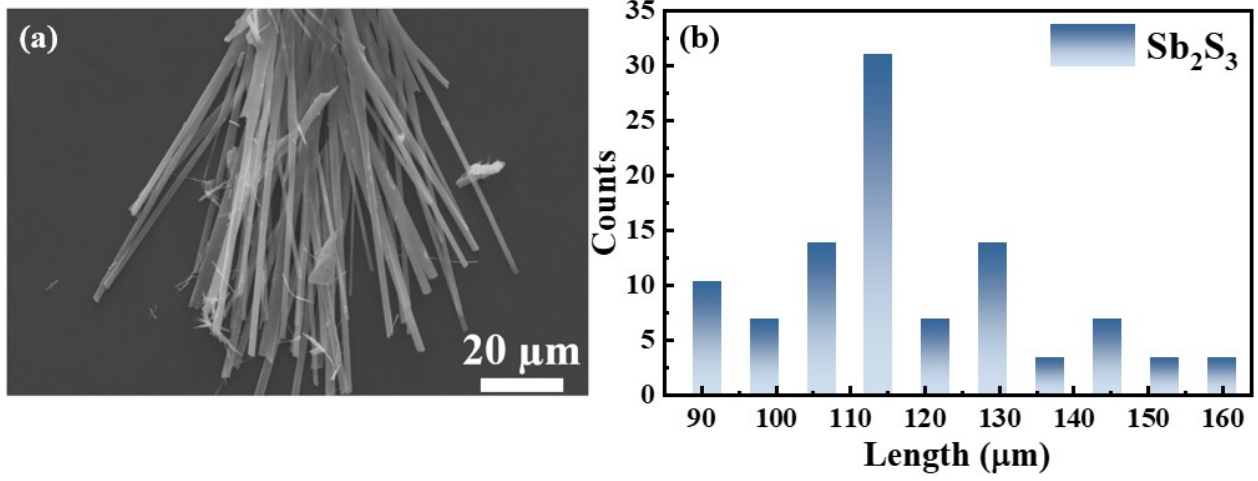


Figure S6. (a) SEM image of Sb₂S₃ microrods; (b) statistical size distribution of length of Sb₂S₃ microrods.

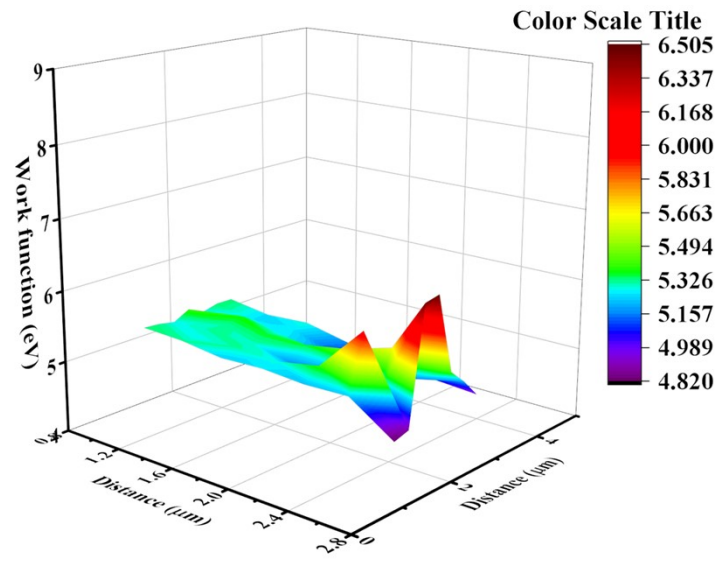


Figure S7. KPFM image of a selected rectangular area measuring $3 \times 3 \mu\text{m}^2$ from a Sb_2S_3 microrod.

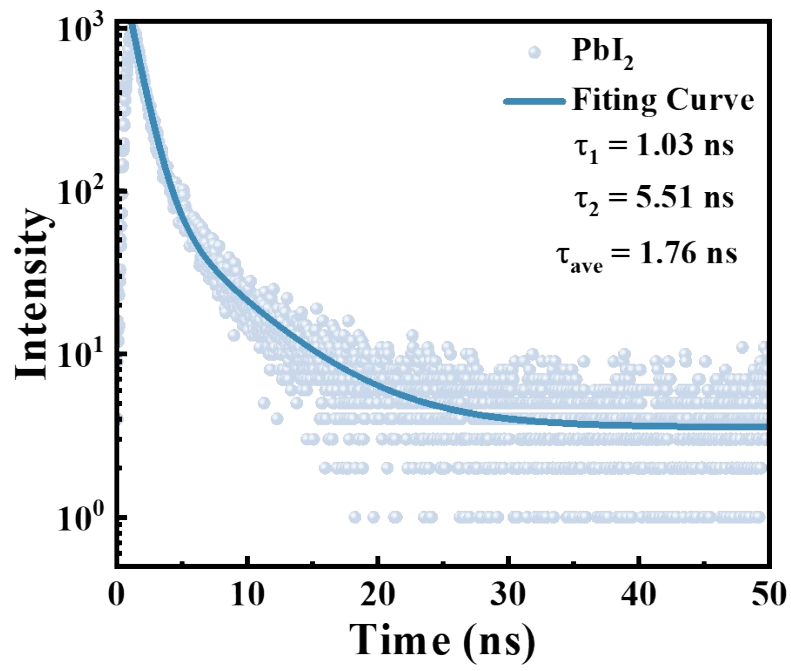


Figure S8. Time-resolved PL (TRPL) spectra of the PbI₂ nanosheets.

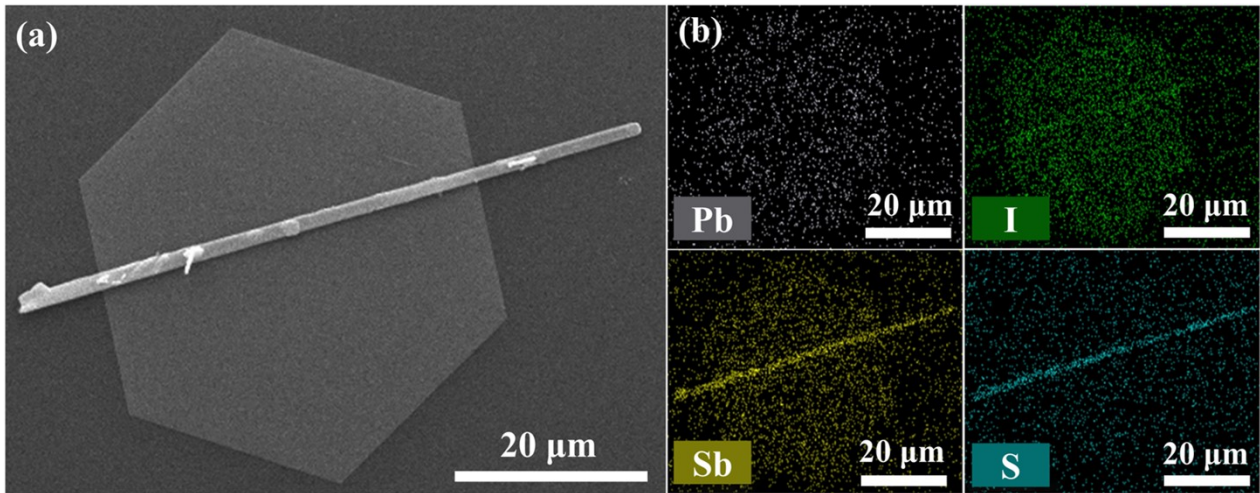


Figure S9. (a) SEM micrograph and (b) corresponding EDX mapping of Pb, I, Sb, and S elements in a 2D/1D $\text{PbI}_2/\text{Sb}_2\text{S}_3$ heterojunction.

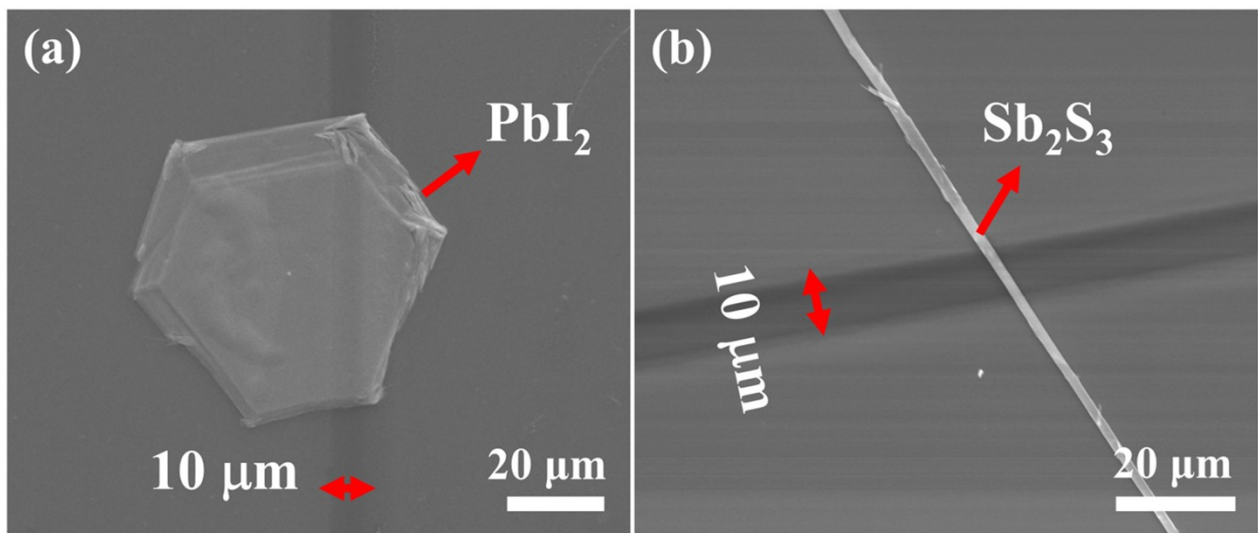


Figure S10. SEM images of (a) a PbI_2 and (b) Sb_2S_3 microrod photodetector device, respectively.

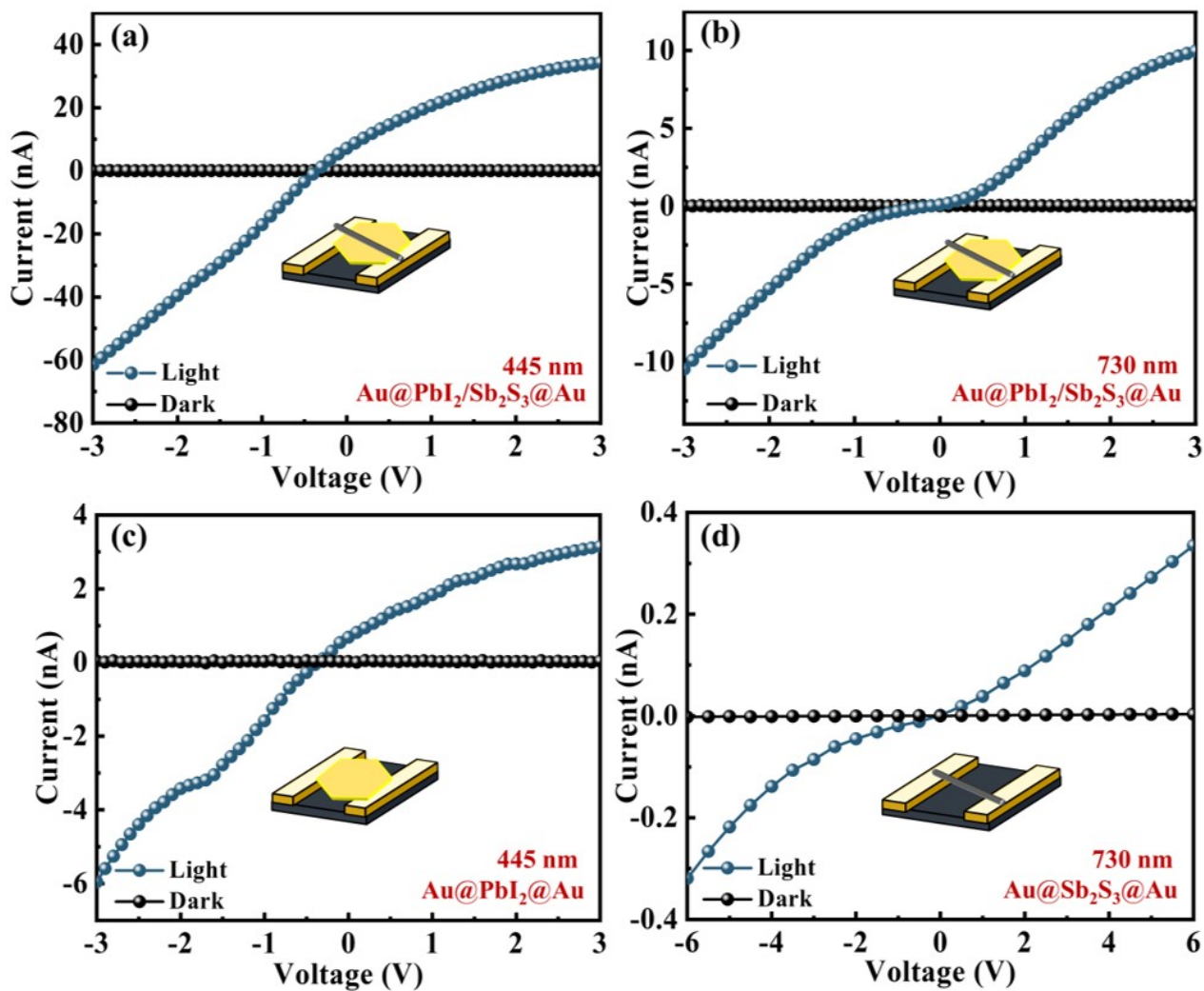


Figure S11. Current-voltage (I - V) curves of the $\text{PbI}_2/\text{Sb}_2\text{S}_3$ photodetector devices measured under dark and (a) 445 nm and (b) 730 nm light illumination, respectively; I - V curves of the (c) PbI_2 nanosheet and (d) Sb_2S_3 microrod photodetector devices measured under 445 nm and 730 nm illumination, respectively.

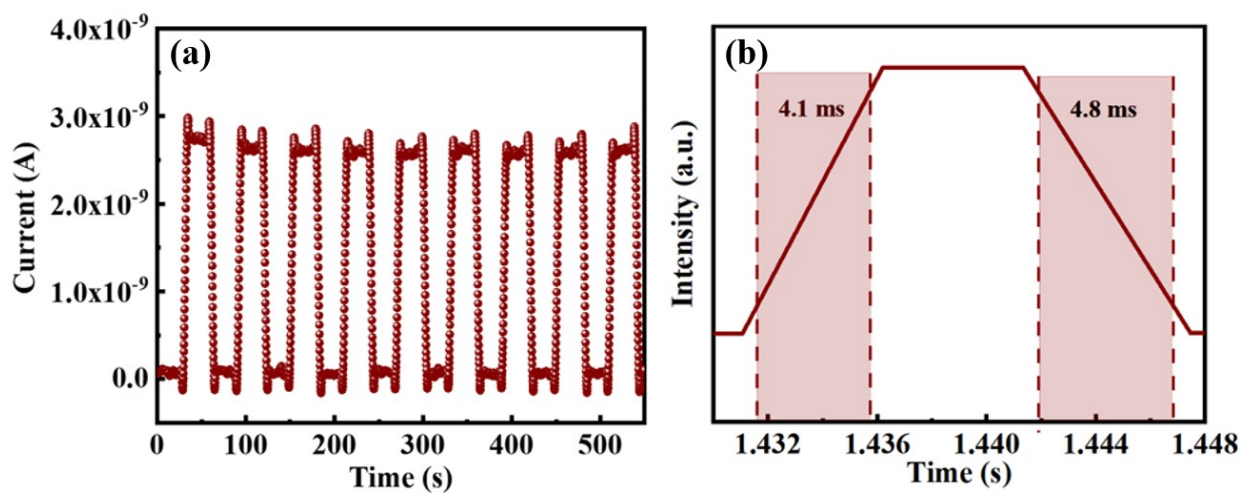


Figure S12. (a) Time-dependent photocurrent and (b) time response curves of an individual PbI_2 nanosheet device measured at 3 V bias under 445 nm monochromatic light.

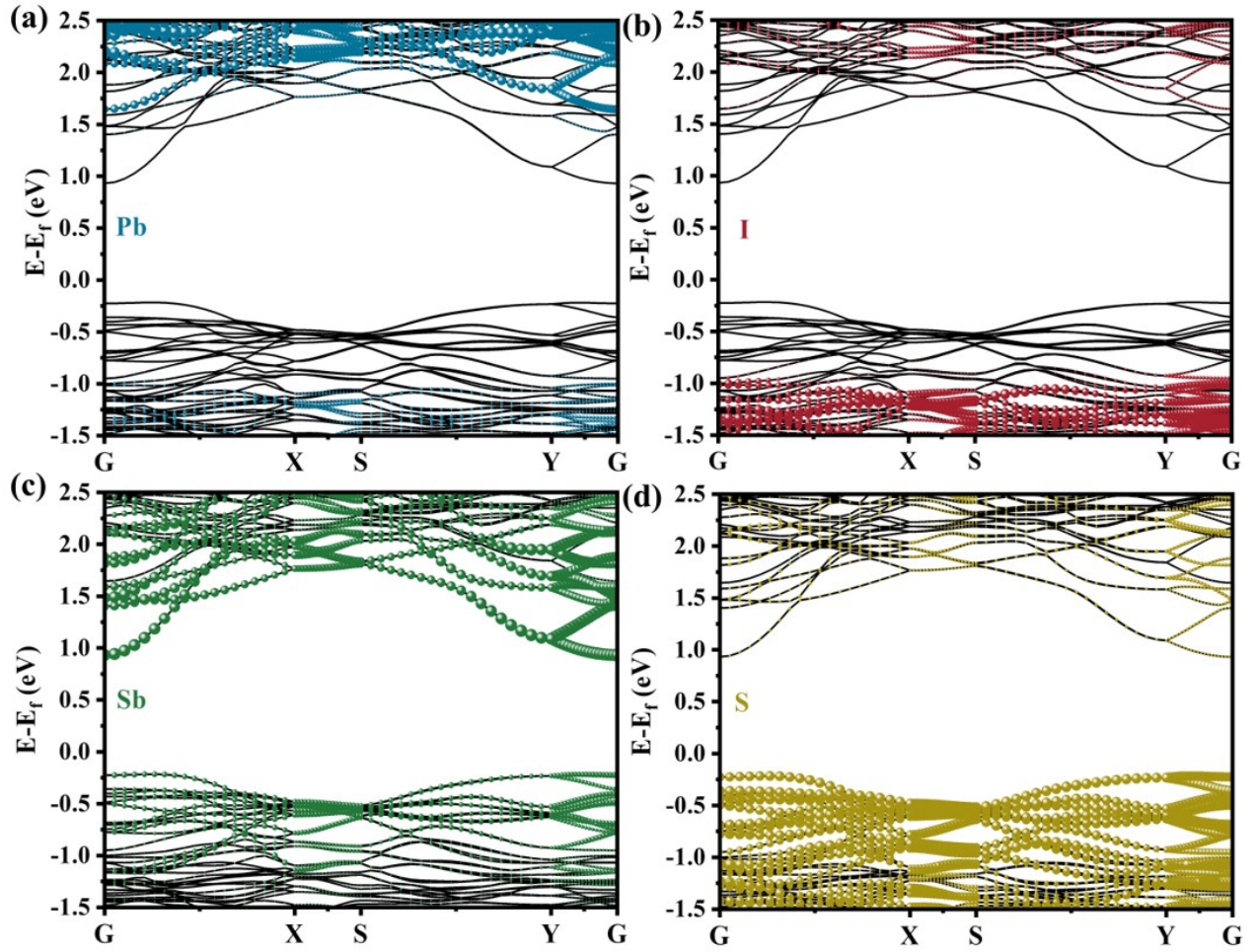


Figure S13. Energy band structure of the $\text{PbI}_2/\text{Sb}_2\text{S}_3$ heterostructure (black curve) with the respective contribution of (a) Pb (blue spheres), (b) I (red spheres), (c) Sb (green spheres), and (d) S (yellow spheres) element highlighted for clarity.